Title

A Collimatorless Detector for In vivo 225Ac Tomography: a Feasibility Study

Authors

Caravaca, Javier
Zheng, Yifan
Huh, Yoonsuk
et al.

Publication Date

2021-10-23

DOI

10.1109/nss/mic44867.2021.9875663

2021 IEEE Nuclear Science Symposium and Medical Imaging Conference (NSS/MIC) | 978-1-6654-2113-3/21/$31.00 ©2021 IEEE | DOI: 10.1109/NSS/MIC44867.2021.9875663

A Collimatorless Detector for In vivo ^{225}Ac Tomography: a Feasibility Study

Javier Caravaca, Yifan Zheng, Yoonsuk Huh, Grant T. Gullberg, Youngho Seo

***Abstract*—Targeted alpha therapy has demonstrated a great efficacy in the treatment of a number of malignancies, but the study of emerging radiopharmaceutical is hindered by the inability of current gamma cameras to image such radiopharmaceuticals in vivo. We use a collimator-less gamma camera consisting of BGO scintillators, multi-channel photomultipliers and an Anger logic circuit to achieve a high sensitivity and obtain planar images of the ^{225}Ac daughters ^{221}Fr and ^{213}Bi for the first time in mice. 0.5 µCi of ^{225}Ac-DOTA-YS5 was injected to a mouse bearing prostate cancer xenografts and imaged 13 days post-injection (0.2 µCi approximated activity). The images reveal the tumor position and the location of other organs with higher uptake. This provides a proof of principle of the power of proximity imaging for ^{225}Ac, and potentially other targeted alpha therapy imaging radionuclides.**

***Index Terms*—preclinical imaging, targeted alpha therapy, actinium-225, proximity imaging**

I. Introduction

Imaging of the targeted alpha therapy (TAT) radioisotope ^{225}Ac [1] would represent a major milestone in the study of radiopharmaceuticals for TAT, a radiotherapy technique that has shown great promise [2, 3]. ^{225}Ac daughters can be imaged through their gamma decays, since two relatively high-energy gamma rays are emitted: a 221 keV from ^{221}Fr and a 440 keV from ^{213}Bi [4]. Nevertheless, this has only been shown for extremely large doses and exposures, and gamma imaging of ^{225}Ac daughters in conditions equivalent to in vivo has never been demonstrated. The alternative options (Cherenkov luminescence imaging [5] and positron emission tomography surrogates [6]) cannot provide a quantitative map of the location of the ^{225}Ac and daughters.

The reason current single photon emission computed tomography (SPECT) devices fail to image ^{225}Ac in vivo is their extremely low sensitivity to high energy gamma rays. The injected doses in TAT are orders of magnitude lower than in other modalities and so, an ultra-high sensitivity is required. Additionally, SPECTs are typically optimized for energies well below 200 keV. Since the main driver of the low sensitivity is the collimator, we propose to image ^{225}Ac in vivo with a collimator-less gamma camera. We use the gamma camera system developed by UC Davis [7] that uses proximity imaging in order to reconstruct the location of the gamma ray sources [8]. This compromises spatial resolution to achieve ultra-high sensitivity, as required by ^{225}Ac imaging for TAT.

Manuscript received December 16, 2021.
This work did not involve human subjects or animals in its research.
J. Caravaca, Yifan, Zheng, Yoonsuk Huh, G. T. Gullberg and Y. Seo are with the Department of Radiology and Biomedical Imaging of the University of California San Francisco in San Francisco (CA) USA.

In this paper, we briefly describe the proximity gamma-ray camera, the reconstruction and the mice tumor models in Sec. II, and we show the first ^{221}Fr and ^{213}Bi images from an ^{225}Ac radiopharmaceutical in vivo in Sec. II-D before concluding in Sec. IV.

II. Methods

A. Proximity camera

Proximity imaging is a modality that relies on the $1/r^2$ dependency of the gamma ray flux, where r is the distance from the gamma ray source. In order to fully benefit from this, the subject needs to be very close (practically in contact) to the detector. UC Davis developed a proximity camera (Fig. 1) that consisted of a collimator-less Anger camera with two detector heads, each with a scintillator optically coupled to a multi-channel photo-multiplier (MC-PMT) and instrumented with pre-amplifiers and an Anger logic circuit [7]. For this experiment, we used two BGO scintillators of $10\,\text{cm}^2 \times 5\,\text{cm}^2$ and 5 mm thickness. The detector heads were covered with two layers of opaque fabric to prevent from light leaks.

For this pilot study, only one MC-PMT ($5\,\text{cm}^2 \times 5\,\text{cm}^2$) was instrumented with an evaluation board for the Domino Ring Sampler [9] version 4, that reads the four channels of the MC-PMT. The trigger was performed by using the self-trigger board functionality, configured to trigger when any of the channels went below a threshold of 0.25 mV.

Waveforms are saved in binary format and analyzed off-line by a custom software. The energy deposited in the detector by the gamma ray interaction is estimated by integrating the waveform below pedestal. The pedestal region is defined by the first 50 samples and the integration region extends from sample 50 to the last (sample 1024). The energy was calibrated with the 662 keV gamma ray emission of a ^{137}Cs source and by fitting the photopeak to a Gaussian distribution. The location of the gamma ray interaction position in the BGO is provided by the Anger logic using the four read-out channels [7].

B. Mouse model

One mouse bearing 22Rv1 [10] prostate cancer subcutaneous xenografts (0.3 – 0.5 cc) was treated with a single 0.5 µCi injection of ^{225}Ac-DOTA-YS5. YS5 is a very promising antibody in clinical trial phase (NCT03575819 and NCT03650491) for prostate cancer [11] and multiple myeloma [12] which binds to CD46, a novel target highly expressed in those malignancies. This radiopharmaceutical being developed at UCSF links YS5 with ^{225}Ac using the DOTA chelator. The mouse was imaged 13 days post-injection, with an estimated activity of 0.2 µCi.

978-1-6654-2113-3/21/$31.00 ©2021 IEEE

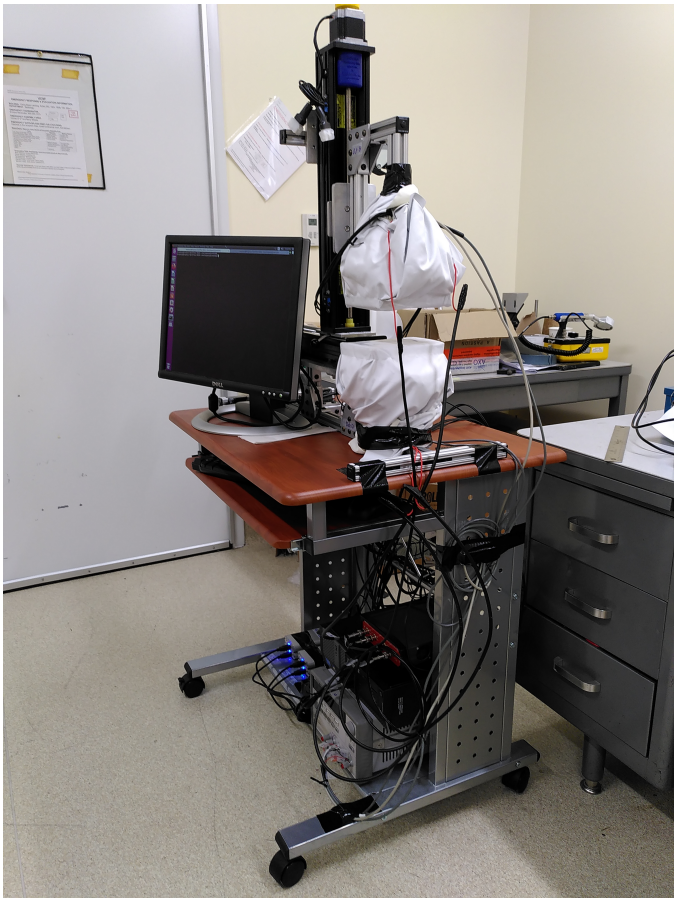

Fig. 1. Proximity camera lent to us by UC Davis, equipped with BGO scintillators.

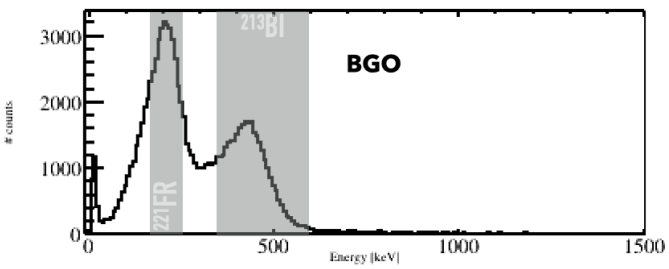

Fig. 2. Energy spectrum collected from ^{225}Ac injected in a mouse in vivo.

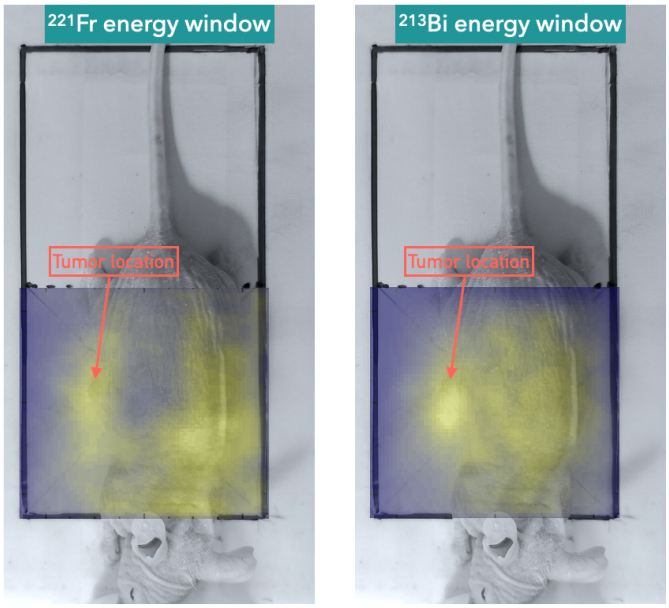

Fig. 3. Images of ^{221}Fr (left) and ^{213}Bi (right) from ^{225}Ac injected in a mouse in vivo.

C. Data acquisition and image reconstruction

The mouse was sedated by administration of isoflurane gas. Once sedated, the mouse was located right over the opaque fabric of the bottom detector head, which is at about 2 mm from the BGO detector, with most of its body within the $5\,\text{mm}^2 \times 5\,\text{mm}^2$ sensitive area. Administration of isoflurane continued for the full imaging session. We collected 100,000 events at about 160 cps in about 10 minutes, after which the mouse was returned to its cage for recovery.

The reconstruction consists on a simple smoothing of the 2D position of the selected gamma ray interactions, using the 5x5 smoothing kernel provided by the ROOT software [13].

D. Imaging results

The ^{221}Fr and ^{213}Bi photopeaks are clearly visible on the spectra obtained with BGO (Fig. 2). ^{221}Fr and ^{213}Bi events are selected based on two different energy windows, (150 keV, 250 keV) and (350 keV, 600 keV), respectively.

Planar images of ^{221}Fr and ^{213}Bi are obtained by applying the smoothing kernel to the 2D distributions of the interactions obtained using the Anger logic for each energy window. The images are shown in Fig. 3 overlaid to a picture of the mouse taken from the top, where the millimeter-size tumor can be appreciated on the left side. The planar images reveal the location of the tumor and the location of other organs with higher uptake like the liver. For the ^{221}Fr image, there is a clear separation between tumor and high-uptake organs. For the ^{213}Bi image, the higher uptake corresponds to the tumor, while there is a less clear separation with respect to the organs. This could be due to differences in the biodistributions of ^{221}Fr and ^{213}Bi, given that they might detach from the targeting agent due to the decay recoil energy and the different chemical properties of the radioisotopes [14].

III. Discussion

This system provides a proof of principle for ^{225}Ac gamma-ray imaging with a collimator-less gamma camera. We show the result with a single MC-PMT and we plan to obtain images of the entire mouse with the full device, that consists of two MC-PMTs at the bottom and two MC-PMTs at the top. These could provide 3D images using a dedicated proximity reconstruction algorithm [8, 15, 16].

The system could benefit from an upgrade in order to overcome the current limitations, namely, poor energy resolution, low read-out rate, and sub-optimal pixel size and gamma-ray interaction location. The use of cadmium zinc telluride (CZT), with a much better energy resolution than BGO, would result in better ^{221}Fr from ^{213}Bi separation as

well as in reduced background noise. CZT could also provide a finer and more reliable pixelization than the current Anger logic, potentially improving image quality. Another important limitation is with the readout system, which induces a dead time and reduces the sensitivity. Modern acquisition systems for CZT detectors eliminate the dead time and maximize sensitivity. Finally, proximity can be combined with Compton imaging in a multi-modality gamma camera. This camera could obtain quantitative 3D images of ^{225}Ac daughters with a sensitivity higher than one order of magnitude with respect to current small animal SPECTs. We designed such system and predicted its performance using with Monte Carlo simulations. That study will be published elsewhere.

IV. Conclusion

Biodistributions of ^{221}Fr and ^{213}Bi have been imaged in vivo after a 10-minutes acquisition with a collimator-less gamma camera designed by UC Davis. These are, to the extent of our knowledge, the first gamma-ray images of ^{225}Ac daughters obtained in vivo. The chosen radiopharmaceutical was the ^{225}Ac-DOTA-YS5, being developed at UCSF, which targets the 22Rv1 tumors induced in a nude mouse. The planar images revealed the position of the tumor and other high-uptake organs for each isotope by separate.

V. Acknowledgments

This work was supported in part by the National Institutes of Health under grant R01 EB026331. The authors thank Gerard Ariño-Estrada and Simon Cherry from the University of California Davis for lending their gamma camera to us. We also thank Kandappa Naidu Bobba and Robert Flavell for their unvaluable help providing us with mice treated with ^{225}Ac. All authors declare that they have no known conflicts of interest in terms of competing financial interests or personal relationships that could have an influence or are relevant to the work reported in this paper.

References

[1] David A Scheinberg and Michael R McDevitt. “Actinium-225 in targeted alpha-particle therapeutic applications”. In: *Current radiopharmaceuticals* 4.4 (2011), pp. 306–320.

[2] Chris C. Parker et al. “Targeted Alpha Therapy, an Emerging Class of Cancer Agents: A Review”. In: *JAMA Oncology* 4 (2018), pp. 1765–1772.

[3] Narges K. Tafreshi et al. “Development of Targeted Alpha Particle Therapy for Solid Tumors”. In: *Molecules* 24.23 (2019). ISSN: 1420-3049.

[4] Andrew KH Robertson et al. “Multi-isotope SPECT imaging of the 225Ac decay chain: feasibility studies”. In: *Physics in Medicine & Biology* 62.11 (2017), p. 4406.

[5] Darpan N. Pandya et al. “Preliminary Therapy Evaluation of ¡sup¿225¡/sup¿Ac-DOTA-c(RGDyK) Demonstrates that Cerenkov Radiation Derived from ¡sup¿225¡/sup¿Ac Daughter Decay Can Be Detected by Optical Imaging for ¡i¿In Vivo¡/i¿ Tumor Visualization”. In: *Theranostics* 6 (2016), pp. 698–709.

[6] Eduardo Aluicio-Sarduy et al. “Production and in vivo PET/CT imaging of the theranostic pair 132/135 La”. In: *Scientific reports* 9.1 (2019), pp. 1–6.

[7] Katherine L Walker, Simon R Cherry, and Gregory S Mitchell. “Detector performance characterization for high sensitivity single-photon imaging”. In: *IEEE transactions on nuclear science* 61.3 (2014), pp. 1118–1125.

[8] Gregory S Mitchell and Simon R Cherry. “A high-sensitivity small animal SPECT system”. In: *Physics in Medicine & Biology* 54.5 (2009), p. 1291.

[9] Stefan Ritt, Roberto Dinapoli, and Ueli Hartmann. “Application of the DRS chip for fast waveform digitizing”. In: *Nuclear Instruments and Methods in Physics Research Section A: Accelerators, Spectrometers, Detectors and Associated Equipment* 623.1 (2010), pp. 486–488.

[10] R Michael Sramkoski et al. “A new human prostate carcinoma cell line, 22R v1”. In: *In Vitro Cellular & Developmental Biology-Animal* 35.7 (1999), pp. 403–409.

[11] Yang Su et al. “Targeting CD46 for both adenocarcinoma and neuroendocrine prostate cancer”. In: *JCI insight* 3.17 (2018).

[12] Daniel W Sherbenou et al. “Antibody-drug conjugate targeting CD46 eliminates multiple myeloma cells”. In: *The Journal of clinical investigation* 126.12 (2016), pp. 4640–4653.

[13] Rene Brun and Fons Rademakers. “ROOT—An object oriented data analysis framework”. In: *Nuclear Instruments and Methods in Physics Research Section A: Accelerators, Spectrometers, Detectors and Associated Equipment* 389.1-2 (1997), pp. 81–86.

[14] Jorgen Elgqvist et al. “The potential and hurdles of targeted alpha therapy–clinical trials and beyond”. In: *Frontiers in oncology* 3 (2014), p. 324.

[15] J Zhou et al. “Maximum a posteriori image reconstruction for a high sensitivity uncollimated small-animal SPECT system”. In: *Fully 3D Image Reconstruction in Radiology and Nuclear Medicine*. 2013, pp. 90–93.

[16] Yifan Zheng et al. “Collimatorless Scintigraphy for Imaging Extremely Low Activity Targeted Alpha Therapy (TAT) with Weighted Robust Least Squares (WRLS)”. In: *International Conference on Medical Image Computing and Computer-Assisted Intervention*. Springer. 2020, pp. 803–811.